Journal of Materials Science: Materials in Electronics (2019) 30:4359–4369
https://doi.org/10.1007/s10854-019-00758-7

REVIEW

Size effect on interface reaction of Sn–*x*Cu/Cu solder joints during multiple reflows

Ru Huang[1] · Haoran Ma[1,2] · Shengyan Shang[1] · Anil Kunwar[1,3] · Yunpeng Wang[1] · Haitao Ma[1]

Received: 29 September 2018 / Accepted: 16 January 2019 / Published online: 1 February 2019
© Springer Science+Business Media, LLC, part of Springer Nature 2019

Abstract

At present, electronic products are developing in the direction of miniaturization and integration, which leads to the downsizing of solder bump in the packaging process. Moreover, micro solder bumps often require undergoing multiple reflow processes due to the improvement of packaging technology, which has a great influence on interface reaction. Hence, it is necessary to study the effects of solder composition, bump size and reflow cycle on interfacial reaction between solder alloys and Cu substrates. In this experiment, Sn–*x*Cu ($x = 0$, 0.7, 2.0 wt%) alloys with diameter of 200 µm, 500 µm, and 800 µm were soldered to Cu substrates at 250 °C for 1 min, and then reflowed 20 cycles totally. The size effect of micro solder joints on the growth of IMC after multiple reflows was analyzed. At the same time, the impact of Cu concentration inside the bulk solder on the interfacial reaction during multiple reflows was explored. This experiment finds that the diameter of IMC grains increases with the decrease of solder ball diameter after one reflow cycle, and a significant size effect occurs in Sn/Cu solder bump. As the number of reflow cycle increases, the size effect on interface reaction is more pronounced. The most direct kinetic factor of this phenomenon is that the average Cu concentration in the small-sized solder ball rises faster than the others. When the number of reflow cycle reach to nine times, the lateral growth rate of IMC grains begins to surpass the longitudinal growth rate, and the morphology of IMC grains becomes flat. This phenomenon is especially evident in the small-sized solder ball. Moreover, the addition of Cu element in solder promotes ripening reaction resulting in the lateral growth of IMC. Cu_6Sn_5 micro particles appearing at the Sn/Cu, Sn–0.7Cu/Cu interface hinder the grain boundary motion and inhibit the lateral annexation of IMC grains, thereby suppressing the lateral growth of IMC.

1 Introduction

As is well known, solder bumps are the most important interconnection method in electronic products; at the same time, they are also the places where reliability is relatively weak. The packaging density is constantly increasing and the size of solder joint is continuously reducing due to the advancement of the semiconductor manufacturing industry, which will cause some new reliability problems [1, 2]. At present, the size of micro solder joints in the flip chip package is decreased to 20–40 µm, which is reduced by one order of magnitude compared to that in the ball grid array structure [3]. At present, it is necessary to perform multiple reflows due to the development of packaging technology and the maintenance requirements of electronic products. Thereby, studying the microstructure evolution of Intermetallic Compounds (IMC) in the solder/substrate interface during multiple reflows is significant to the development of package interconnection technology.

In current study, the number of reflow times is set as five cycles and there are few studies about the effect of more reflow cycles on the interfacial reaction. Ha et al. studied the growth of IMC at the Sn–2.5Ag/Cu interface during multiple reflows. It was found that the Cu_6Sn_5 phase IMC layer appears at the interface after one reflow cycle. The thickness of the IMC increases with the number of reflow cycles increases. After the fifth reflow cycle, the scalloped Cu_6Sn_5 layer and the Cu_3Sn thin layer can be found simultaneously [4].

✉ Haoran Ma
mhr@mail.dlut.edu.cn

Haitao Ma
htma@dlut.edu.cn

1 School of Materials Science and Engineering, Dalian University of Technology, Dalian 116024, China

2 School of Microelectronics, Dalian University of Technology, Dalian 116024, China

3 Department of Materials Engineering, KU Leuven, Kasteelpark Arenberg 44, 3001 Heverlee, Belgium

The concentration and distribution of elements in solder bumps will change significantly during the soldering process due to the mutual diffusion of elements, which will cause the change of IMC morphology. This phenomenon is particularly noticeable in the small-sized solder bumps [5]. It is important to study the effect of the initial Cu concentration in bulk solders and the change of Cu concentration in the solder bumps on IMC growth during multiple reflows. Chang et al. studied the interfacial reaction in Sn–3Ag–*x*Cu ($x=0.3$, 0.5, 0.7 wt%) solder bump with ball diameter of 400, 500, 760 and 900 μm. It was found that the size of Cu_6Sn_5 grains at the interface increases with the decrease of solder balls diameter [6]. Ma et al. used Sn, Sn–0.5Cu, Sn–0.7Cu, Sn–1.5Cu, and Sn–2.0Cu solder to study the effect of Cu content in solder on IMC growth. It is considered that the addition of Cu element in the solder can promote the ripening reaction of IMC grains [7].

This research aimed at studying the size effect on interface reaction of Sn/Cu solder joints during multiple reflows and the effect of Cu content on IMC growth at Sn–*x*Cu/Cu interface. The morphology of IMC was obtained by scanning electron microscopy (SEM). In order to analyze the effect of average Cu concentration in solder bump on the growth of IMC during multiple reflows, the average Cu concentration was obtained by combining high-pressure (HP) air purging experiment and electron microprobe (EPMA). These results can provide reasonable data for reliability analysis during the actual packaging process.

2 Experimental procedures

Sn–*x*Cu ($x=0$, 0.7, 2.0 wt%) alloys and Cu sheets were used in this experiment. The purity of raw materials Sn and Cu were 99.95% and 99.99% respectively. Sn and Cu were mixed in according to their mass percentages and then put into a vacuum tube furnace. The temperature was raised to 500 °C under the protection of argon atmosphere and kept for 5 h to mix Sn, Cu uniformly and then cooled to room temperature with furnace. Afterwards, the obtained solder was fabricated into solder balls with the diameter of 200 μm, 500 μm, and 800 μm.

The dimensions of Cu sheets were 15 mm × 5 mm × 100 μm. The oxide film on Cu sheets was washed with 5 vol% HCL solution, then rinsing Cu sheets with alcohol. A layer of flux (AMTECH:NC-559-ASM) was applied to the cleaned Cu sheets for soldering. This study was carried out in a heating furnace. Each sample was soldered at the temperature of 250 °C for 1 min and then reflowed 20 cycles totally. The air cooling rate is around 7.4 °C/s.

The HP air purging device was used in this experiment to obtain the morphology of IMC at isothermal heating stage, as shown in Fig. 1. The high pressure nozzle aligning with the liquid solder was used to release compressed air after the end of the isothermal heating stage. As a result, the solder layer on the Cu substrate was quickly purged and then IMC morphology of the isothermal heating stage can be obtained. In addition, the blown solder was collected, and the concentration of Cu in the solder bump can be measured by electron microprobe (EPMA-1600) to study the influence of Cu concentration in solder bulk on interface reaction during isothermal heating stage. The purging device selected for this experiment was a 2530 oil-free air compressor and the rated gas pressure was set as 0.8 MPa.

In order to obtain the cross-sectional morphology of IMC, 5 vol% HNO_3 + 2 vol% HCL + 93 vol% C_2H_2OH solution was utilized to the samples. The top-view morphology of interfacial IMC was presented by 10% vol% HNO_3 aqueous solution. These samples were ultrasonically cleaned with alcohol to remove residual solder from the interface, after that the morphology of interfacial IMC to can be fully exposed. The morphology of interfacial IMC was observed by SEM [Zeiss Supra 55(VP)]. And the data is measured by Image-pro plus and Photoshop. The average IMC thickness was expressed by S/L, where S is the IMC area and L is the interface width.

3 Results and discussion

3.1 Size effect of Sn/Cu interface reaction during multiple reflows

Figures 2 and 3 present the SEM images for top-view observation of IMC at Sn/Cu interface, and the diameter of Sn solder balls is 200 μm, 500 μm, 800 μm respectively. It can be found that the morphology of Cu_6Sn_5 grains generating at the soldering interface is prismatic after one reflow cycle. The morphology of Cu_6Sn_5 grain turns from prismatic to scalloped during multiple reflows. Results in Fig. 4 indicate that the diameter of Cu_6Sn_5 grains becomes larger during

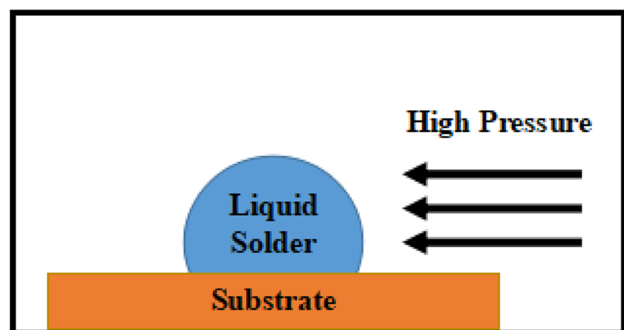

Fig. 1 Schematic diagram of HP air purge experiment

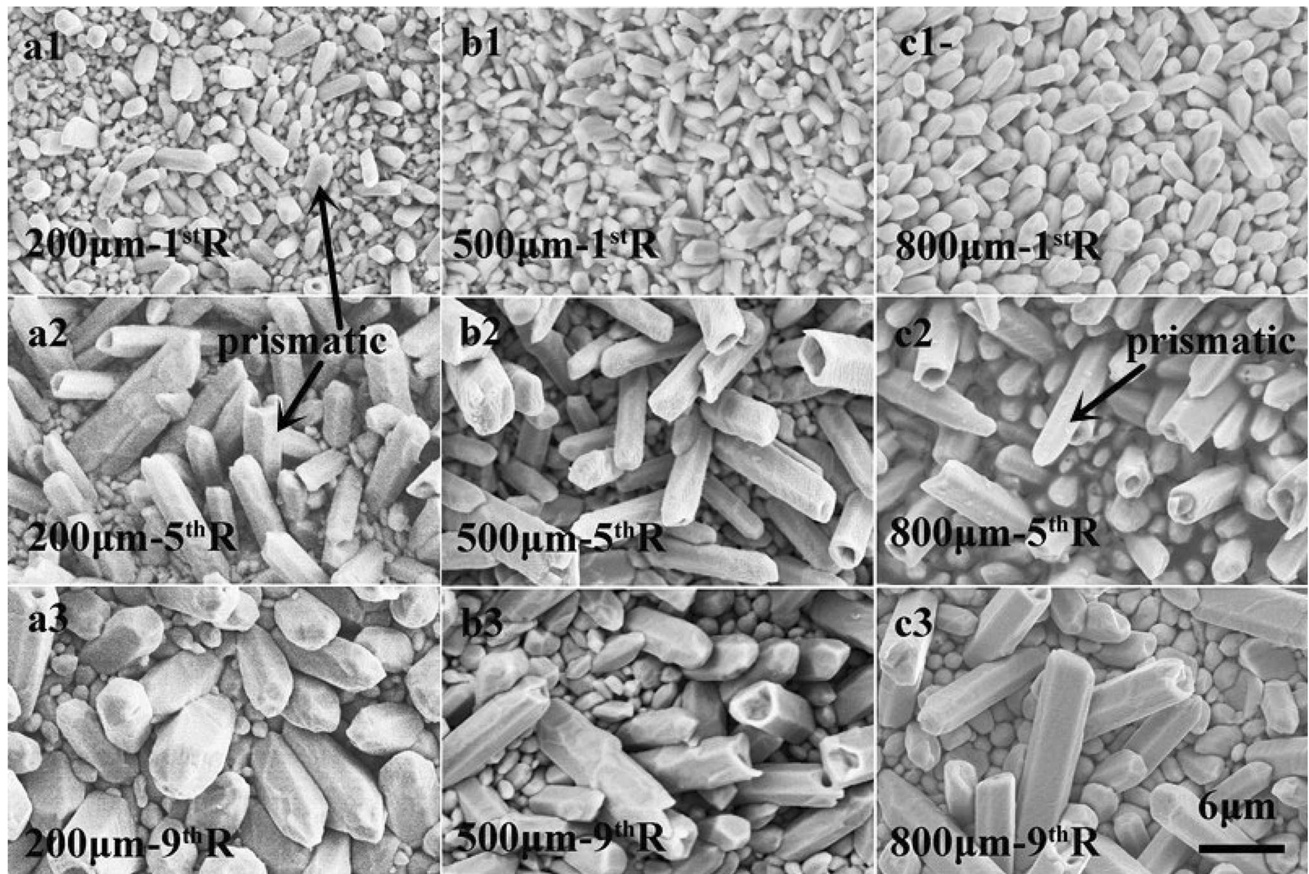

Fig. 2 Top-view morphology of Cu_6Sn_5 grains at Sn/Cu interface before the ninth reflow cycle

multiple reflows. The gap between grains is gradually filled, and the number of Cu_6Sn_5 grains decreases.

From Table 1, it can be found that the diameter of Cu_6Sn_5 grains in solder bump with ball diameter of 200 μm, 500 μm, 800 μm after one reflow cycle has a relationship of 200 μm > 500 μm > 800 μm. The significant size effect on interface reaction appears. The growth rate of IMC grains diameter is the largest in Sn/Cu solder bump with solder ball diameter of 200 μm, and the lowest at the interface of 800 μm solder balls. The growth rate of IMC grains diameter in the solder bump with ball diameter of 200 μm is twice than that with the balls diameter of 800 μm. There is an obvious size effect on the grains morphology at interface during multiple reflows.

The saturated solubility of Cu atoms in Sn solder is 1.6 wt% at 250 °C [8]. During the actual reflow process, the Cu concentration in the solder bump is constantly changing. In order to study the effect of Cu concentration on interface reaction, the average Cu concentration in Sn/Cu solder layer during multiple reflows was measured, as shown in Fig. 5.

Cu concentration in Sn/Cu solder layer with ball diameter of 200 μm increases the fastest under the first reflow due to the shortest diffusion distance, which lead to the less number of Cu_6Sn_5 grains and the large grains size at Sn/Cu interface. Because of the longest diffusion distance in Sn/Cu solder layer with ball diameter of 800 μm, the Cu concentration increases the slowest in 800 μm solder balls under the first reflow. As the result, the diameter of IMC grains in solder bump with ball diameter of 200 μm is the largest, and the diameter of IMC grains in 800 μm solder bump is the smallest.

The Cu atoms in the large-sized solder bump reach a saturation concentration for a longer time than that in the small-sized solder bump during multiple reflows. The diffusion distance of the small-sized solder bump is short [9], and the precipitated Cu_6Sn_5 particles are more likely to diffuse to the interface and adhere to the already formed IMC resulting in the growth of IMC grains diameter. Therefore, the effect of reflow times on grains diameter in the large-sized solder bump is less than that in the small-size solder bump, which will promote the growth of grains diameter in the small-sized solder bump under multiple reflows.

It is well known that the growth of interfacial grains is controlled by both ripening reaction and interface reaction [10]. A sketch, explaining the growth mechanism of IMC, is drawn in Fig. 6. The IMC growth flux J_g is mainly

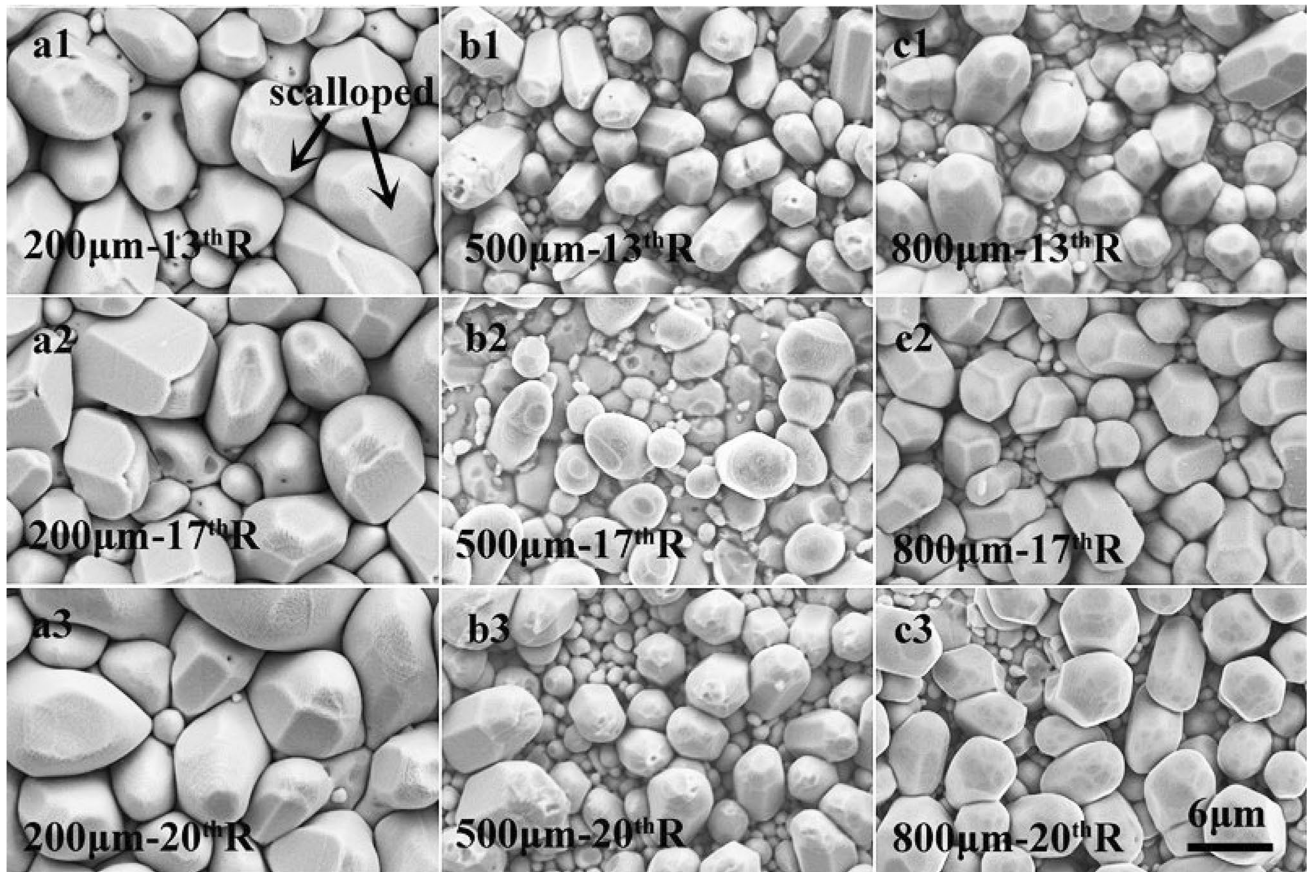

Fig. 3 Top-view morphology of Cu_6Sn_5 grains at Sn/Cu interface after the ninth reflow cycle

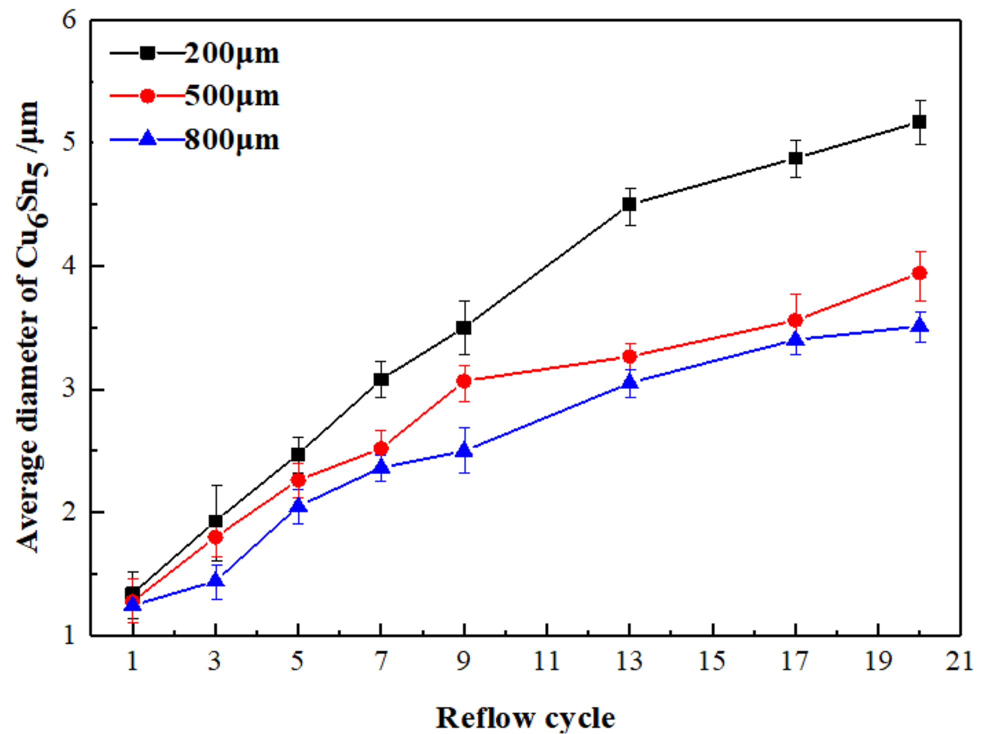

Fig. 4 Average diameter of Cu_6Sn_5 grain at Sn/Cu interface during multiple reflows

Table 1 Cu_6Sn_5 grain diameter and their growth rate in Sn/Cu solder bump with different solder ball diameter

Solder ball diameter (μm)	200	500	800
Cu_6Sn_5 grains diameter after the first reflow (μm)	1.34	1.28	1.24
The growth rate of Cu_6Sn_5 grains diameter after the 20th reflow cycle (μm/cycle)	0.22	0.14	0.12

constituted by five Cu diffusion fluxes [11]. (1) volume diffusion: $J_{in\text{-}a}$; (2) grain boundary diffusion: $J_{in\text{-}b}$; (3) bulk diffusion in liquid solder: $J_{IMC/solder}$; (4) deposition reaction: $J_{solder/IMC}$; (5) ripen diffusion: J_R, this flux mainly positive to change IMC grain diameter, and negative to control the IMC thickness. The annexation behavior between grains occurs during isothermal heating stage. During the cooling process, Cu_6Sn_5 grains grow in a direction of perpendicular to the substrate substantially [12].

$$J_g = J_{in\text{-}a} + J_{in\text{-}b} - J_{IMC/solder} + J_R + J_{solder/IMC} \quad (1)$$

As shown in Fig. 7 and Table 2, the growth rate of IMC thickness is less than the growth rate of Cu_6Sn_5 diameter after the ninth reflow cycle, especially in solder balls with the diameter of 200 μm. In this study, the growth rate of IMC thickness is represented as the longitudinal growth rate of Cu_6Sn_5 and the growth rate of grains diameter is represented as the lateral growth rate of Cu_6Sn_5 grains. After the ninth reflow cycle, no matter what size the solder diameter it is, the lateral growth rate was larger than the longitudinal growth rate of Cu_6Sn_5 grains at the interface. Moreover, the thicker IMC layer has been formed after the ninth reflow cycle, the Cu atom diffusion channel becomes narrower. As a result, the thicker IMC layer blocks the dissolution of Cu atoms into the solder layer and hinders the diffusion of Cu atoms, the flux of $J_{in\text{-}b}$ and $J_{in\text{-}a}$ decreases. IMC thickness increases slowly because the growth flux of IMC mainly comes from $J_{Solder/IMC}$ [13]. The dissolution rate of Cu from the substrate to the solder decreases after the ninth reflow cycle, and the Cu-rich region will be formed near the

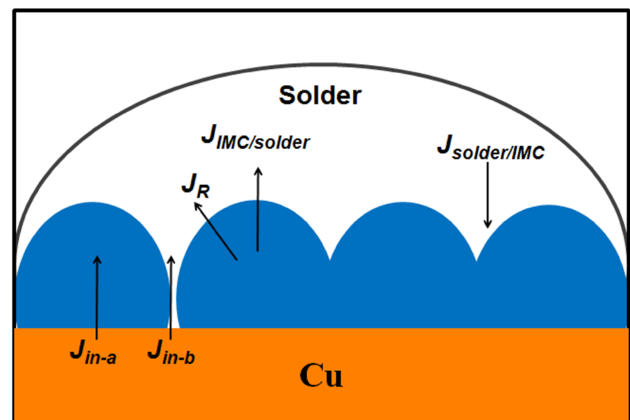

Fig. 6 Schematic diagram for IMC growth model

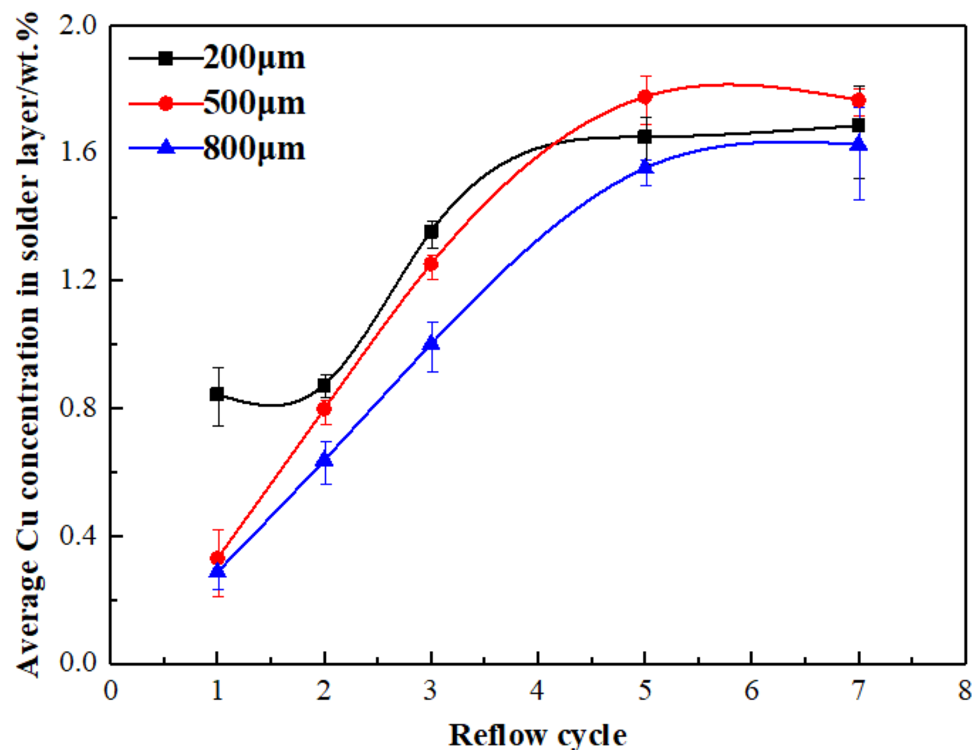

Fig. 5 Average Cu concentration in solder layer with different ball diameter in Sn/Cu solder layer during multiple reflows

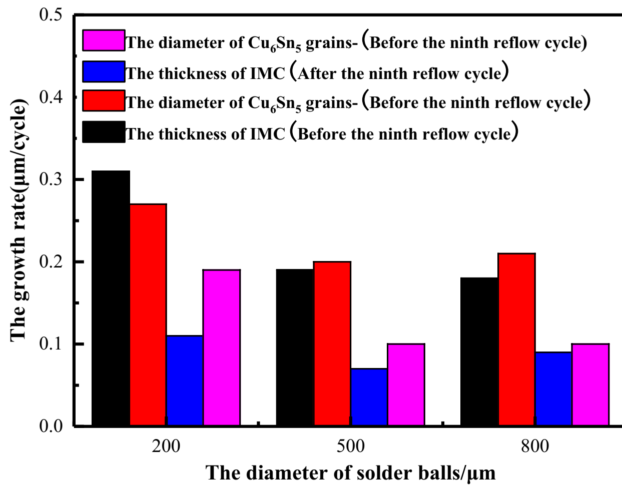

Fig. 7 The growth rate of IMC thickness and Cu_6Sn_5 grains diameter at Sn/Cu interface during multiple reflows

Table 2 The growth rate of IMC thickness and diameter at Sn/Cu interface after the ninth reflow cycle

Solder ball diameter	200	500	800
The growth rate of IMC thickness (μm/cycle)	0.11	0.07	0.09
The growth rate of Cu_6Sn_5 grains diameter (μm/cycle)	0.19	0.10	0.10

interface, which promoted the ripening reaction. Therefore, the lateral growth rate of IMC grains is faster than the longitudinal growth rate after the ninth reflow cycle, especially for the small-sized solder ball. That is because the amount of Sn in the small-sized solder ball is small. It is difficult to precipitate enough Cu_6Sn_5 grains to the interface after the ninth reflow cycle.

3.2 Size effect of Sn–*x*Cu/Cu interface reaction during multiple reflows

It is known that Cu atoms in the substrate and the Sn atoms in the solder bulk will mutually diffuse during reflow process [14]. It has been discussed above that the size of the solder joints affects the Cu concentration in the solder layer, further more affecting the growth behavior of IMC. Moreover, the effect of the initial Cu concentration in micro solder balls on interface reaction will be further studied.

At Sn–0.7Cu/Cu and Sn–2.0Cu/Cu interface, the Cu atoms in the Cu_6Sn_5 grains are derived not only from the substrate but also from the solder itself. Figures 8 and 9 present the SEM images of IMC at Sn–*x*Cu/Cu interface, and the diameter of Sn–*x*Cu solder balls is 200 μm. As is shown in Figs. 8 and 9, the morphology of IMC layer at the Sn/Cu interface is relatively irregular, IMC grains morphology is fine prismatic, and the average diameter of IMC grains at Sn/Cu interface is smaller than the others. More uniform scalloped IMC grains are produced at Sn–2.0Cu/Cu interface after one reflow cycle, and the average diameter of Cu_6Sn_5 grains at Sn–2.0Cu/Cu interface is the largest, which is three times larger than that at Sn/Cu interface. It can be seen from Table 3 that the growth rate of Cu_6Sn_5 grain diameter at the Sn–2.0Cu/Cu interface is much higher than that at Sn/Cu and Sn–0.7Cu/Cu interface.

The increase of initial Cu concentration in solder balls makes IMC grains morphology more uniform and continuous, grains morphology grows toward the spheroid during multiple reflows, as is shown in Fig. 10. It can be concluded that the addition of Cu promotes the ripening reaction of IMC grains.

In order to describe the three-dimensional morphology of the grains, researchers introduce the concept of aspect ratio. The aspect ratio of IMC grain is defined by grain diameter/height, which is calculated through IMC diameter/thickness in this article. When aspect ratio's value is 2, the morphology of interfacial grains is hemispherical;

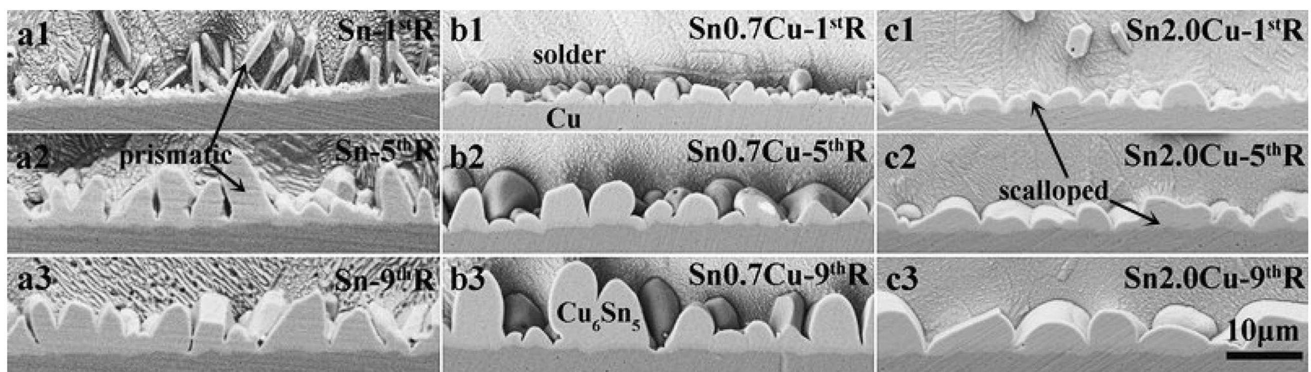

Fig. 8 Cross-sectional morphology of IMC in Sn–*x*Cu/Cu bump with ball diameter of 200 μm during multiple reflows

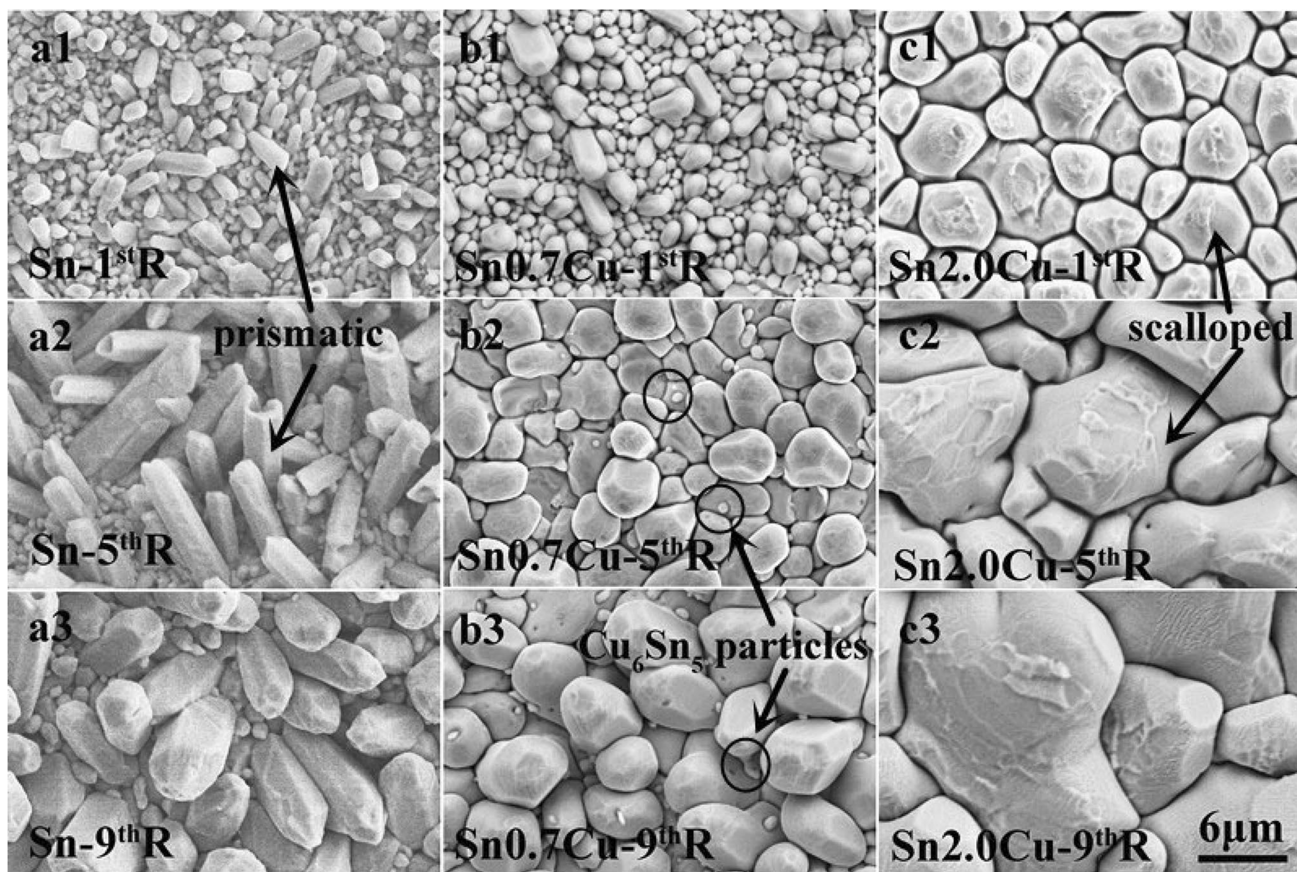

Fig. 9 Top-view morphology of IMC grains in Sn–*x*Cu/Cu bump with ball diameter of 200 μm before the ninth reflow cycle

Table 3 Cu_6Sn_5 grains diameter and their growth rate in Sn–*x*Cu/Cu bump with ball diameter of 200 μm

Solder ball composition	Sn	Sn–0.7Cu	Sn–2.0Cu
Cu_6Sn_5 grains diameter after one reflow cycle (μm)	1.34	1.42	4.62
The growth rate of Cu_6Sn_5 grains diameter after the 20th reflow cycle (μm/cycle)	0.22	0.23	0.66

when aspect ratio's value is > 2, the morphology of interfacial grains is flat scallop; when aspect ratio's value is < 1, the morphology of interfacial grains tends to be prismatic. The value of the aspect ratio can only describe the change process of grains morphology [15].

According to Fig. 11, the morphology of IMC grains is always flat and scalloped-like at Sn–2.0Cu/Cu interface during multiple reflows, because its aspect ratio fluctuates around value 2. The lateral growth rate of IMC grains is greater than the longitudinal growth rate. The aspect ratio of IMC grains at Sn–Cu/Cu and Sn–0.7Cu/Cu interface is less than value 1 during multiple reflows, and the morphology of grains is slender. The fluctuation of aspect ratio is not significant with the increase of reflow cycles. This indicates that the reflow cycle influences the average diameter and thickness of IMC grains, but it has no influence on the morphology of the Cu_6Sn_5 grains.

The Cu concentration in Sn–2.0Cu/Cu solder layer is supersaturated at 250 °C, and the diffusion rate of Cu atoms into the solder is small. Therefore, a Cu-rich region is formed at the near interface to promote the ripening reaction of grains. However, the size of Cu_6Sn_5 grains at Sn–0.7Cu/Cu interface does not increase significantly.

It can be seen from the top-view images of Figs. 9 and 10 that a large number of particles were found in Sn–0.7Cu/Cu interface, while no small particles were found at Sn–2.0Cu/Cu interface. It was verified that these small particles are all Cu_6Sn_5 by EDX [7]. It is apparent that these small particles do not grow from the soldering interface, but attach on the surface of the large Cu_6Sn_5 grains. Figures 12 and 13 shows

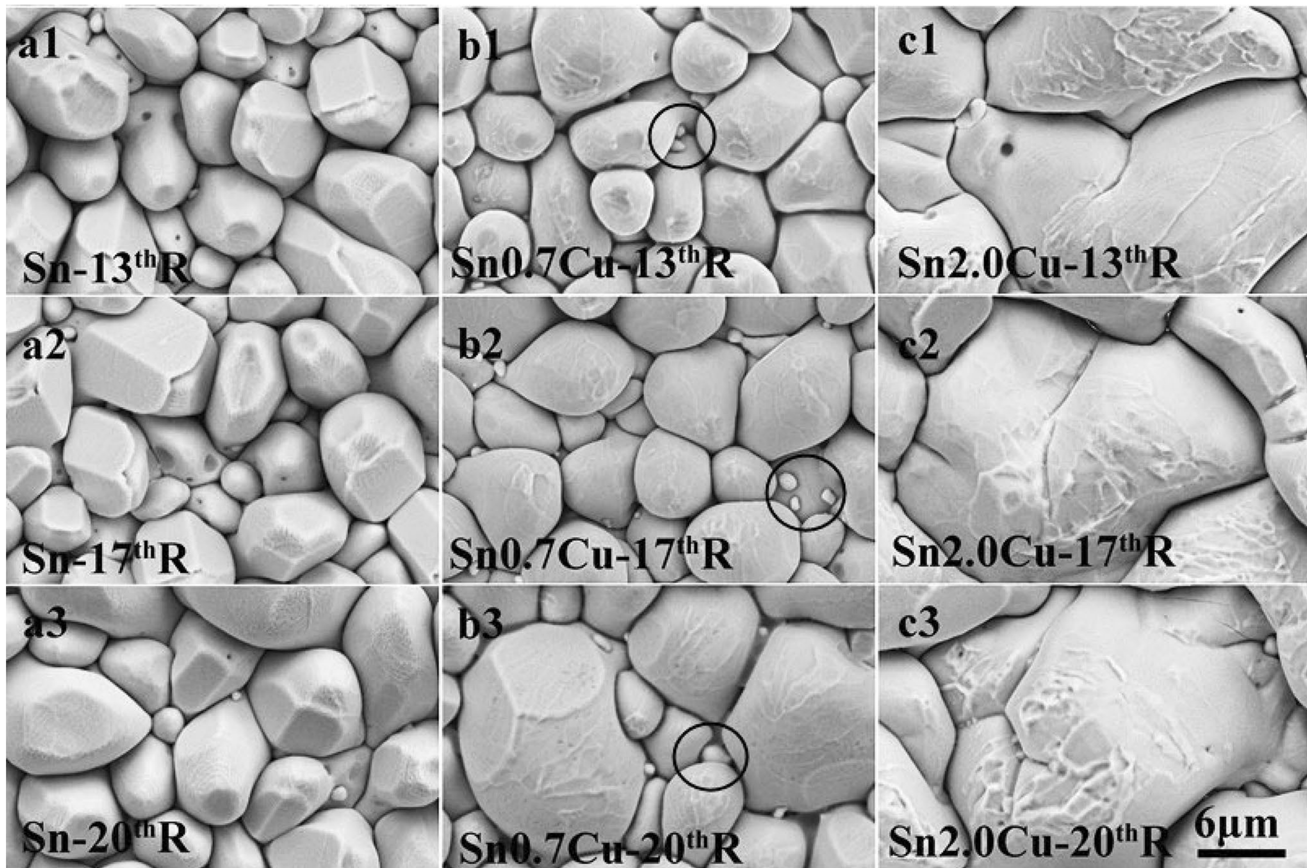

Fig. 10 Top-view morphology of IMC grains in Sn–*x*Cu/Cu bump with ball diameter of 200 μm after the ninth reflow cycle

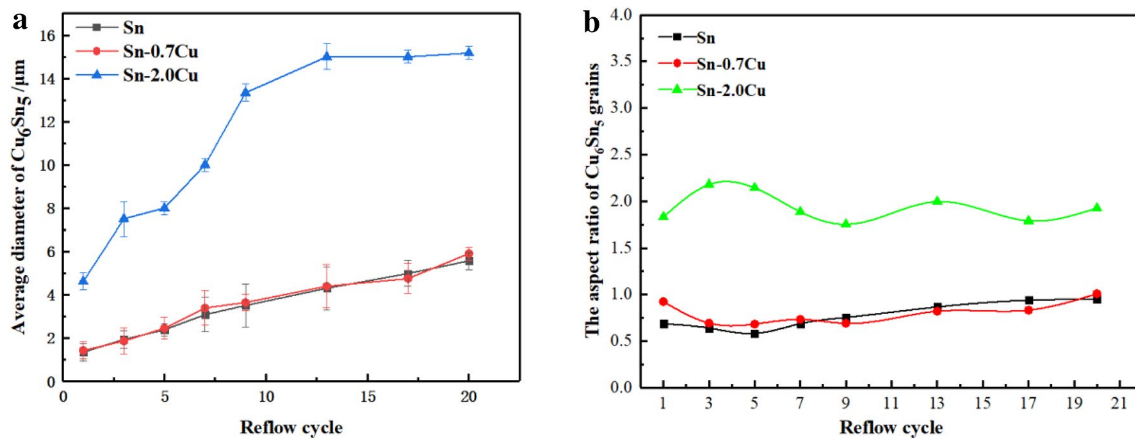

Fig. 11 IMC size evolution with reflow cycles at Sn–*x*Cu/Cu interface: **a** the diameter of IMC grains; **b** the aspect ratio of IMC grains

the top-view of IMC grains morphology in Sn–0.7Cu/Cu bump with solder ball diameter of 200 μm, 500 μm, 800 μm at isothermal heating stage. It can be found that these Cu_6Sn_5 particles will not only deposit on the surface of the grains during cooling, but also attach on the substrate during isothermal heating stage. These Cu_6Sn_5 particles still exist and grow up during multiple reflows. Figure 13 demonstrates that some small particles are attached to the original Cu_6Sn_5 grains, which will cause the change of original grains morphology during multiple reflows. The original grains tend to bypass these particles to grow, such as particle 1, particle 2 and particle 3.

This phenomenon is very similar to the IMC growth at Sn–Ag/Cu interface. Figure 14 present the SEM images of IMC grains at Sn/Cu and Sn–3.5Ag/Cu interface [16]. As is shown in Fig. 14c, there are many Ag_3Sn particles landing onto the surface of IMC grains. These Ag_3Sn particles reduce the surface energy of IMC grains and block the annexation between the adjacent Cu_6Sn_5 grains resulting in the shielding effect on the lateral growth of IMC [16, 17]. In addition, Ag_3sn particles at the grain boundaries protect the diffusion channels between grains from being filled, which promotes the longitudinal growth of IMC. Compared with the diameter of IMC grains at Sn/Cu interface, the IMC grains diameter in Sn–0.7Cu/Cu solder bump does not increase significantly, that probably due to the presence of many small Cu_6Sn_5 particles on the original IMC.

According to the experimental results, the morphology of IMC at Sn–*x*Cu/Cu interface are simply drawn in Fig. 15. The small particles adsorbed on the substrate act as nucleation sites to increase the nucleation rate at the soldering interface. During the cooling stage, these particles grow and compete with the original Cu_6Sn_5 grains for the limited growth space. The growth of grains causes interactions between small particles and original Cu_6Sn_5 grains, which distort the morphology of the original grains.

In Sn–0.7Cu/Cu solder bumps, Cu_6Sn_5 phase as the second phase tends to adsorb on the primary phase β–Sn to form eutectic structures, which are Cu_6Sn_5 particles in the

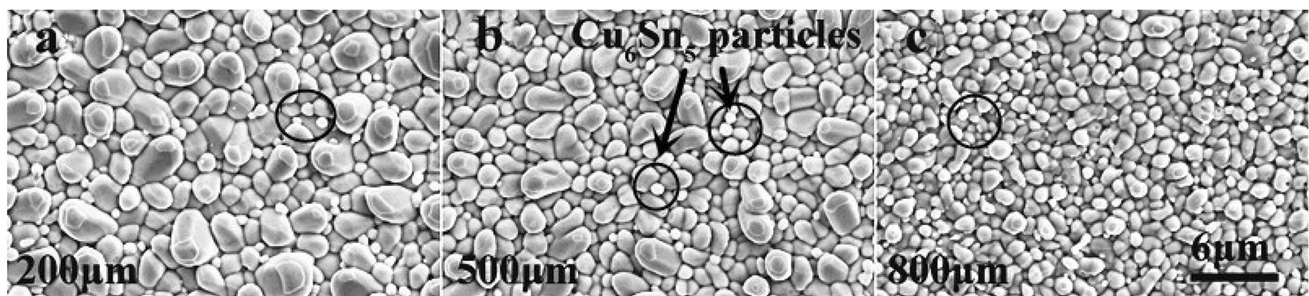

Fig. 12 Top-view morphology of IMC grains in Sn–0.7Cu/Cu bump at isothermal heating stage after one reflow cycle

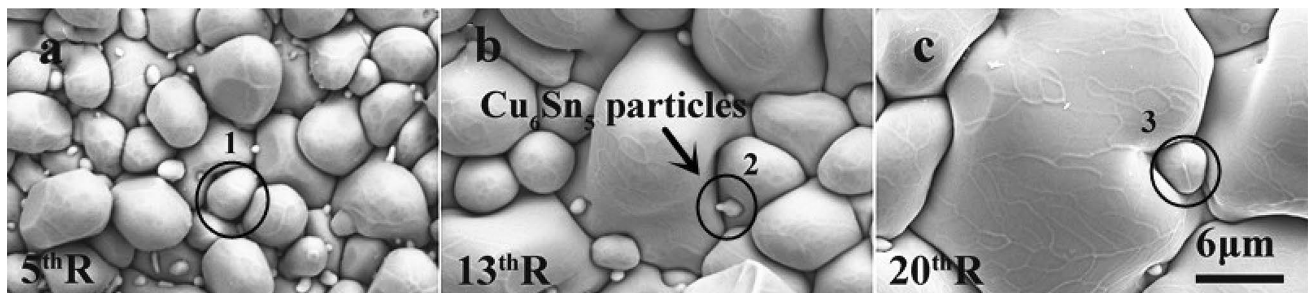

Fig. 13 Top-view morphology of IMC grains in Sn–0.7Cu/Cu bump with ball diameter of 500 μm at isothermal heating stage after multiple reflows

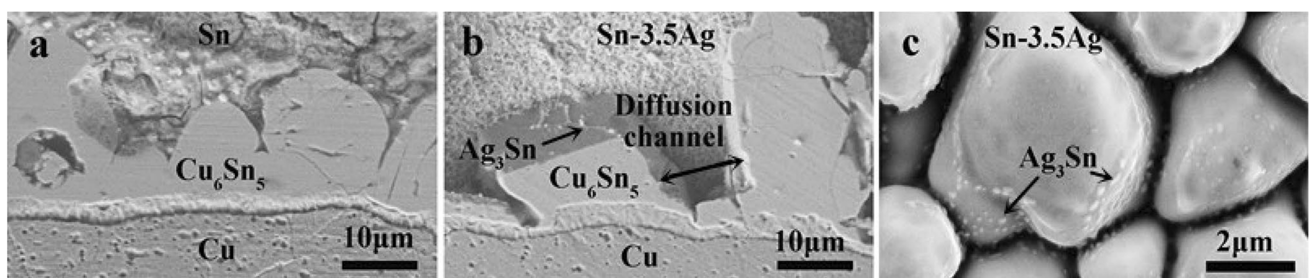

Fig. 14 SEM images showing the IMC grains after the second reflow cycle: **a** cross-sectional of IMC at Sn/Cu interface; **b** cross-sectional of IMC at Sn–3.5Ag/Cu interface; **c** top-view of IMC grains at Sn–3.5Ag/Cu interface

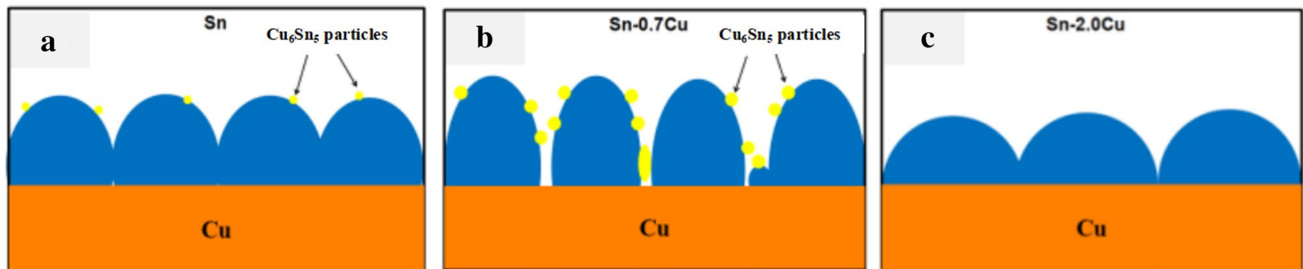

Fig. 15 A sketch showing the IMC morphology in Sn–*x*Cu/Cu solder bumps

above Figure [18, 19]. These particles, as heterogeneous phase nucleation site, tend to inhibit boundary motion and hinder the lateral annexation behavior. In addition, small particles at the grain boundaries protect the diffusion channels between grains. During the cooling stage, the filled rate of grains at the gap slows down. Cu atoms on the substrate can continue to pass through the grain boundaries to reach the solder layer, thereby promoting the longitudinal growth of the interfacial IMC layer.

Cu_6Sn_5 particles are directly precipitated in the Sn–2.0Cu/Cu solder bump at 250 °C. Due to the long super saturation time of Cu atoms in Sn–2.0Cu/Cu solder bump, the precipitated Cu_6Sn_5 particles have sufficient growth conditions, then these particles grow up and mutual annexation during isothermal heating stage. Therefore, Cu_6Sn_5 particles are not found in Sn–2.0Cu/Cu solder bump. In summary, the relationship in the growth rate of IMC grains diameter at Sn–*x*Cu/Cu interface is: Sn–2.0Cu > Sn > Sn–0.7Cu, and the relationship in IMC thickness growth rate at Sn–*x*Cu/Cu interface is: Sn–0.7Cu > Sn > Sn–2.0Cu.

4 Conclusion

The conclusions related to the study on size effect on IMC grains growth are outlined as following:

(1) After one reflow cycle, the diameters of IMC grains in Sn/Cu solder bump with solder ball diameter of 200 µm, 500 µm, 800 µm are 1.34 µm, 1.28 µm, 1.24 µm, respectively. This experiment shows that the diameter of IMC increases with the decrease of solder ball diameter after one reflow cycle, which shows significant size effect on IMC growth.

(2) As the number of reflow cycle increases, the size of IMC becomes bigger and the size effect on interface reaction is more pronounced. The growth rate of IMC gains diameter in Sn/Cu solder bump with solder ball diameter of 200 µm, 500 µm, 800 µm is 0.22 µm/cycle, 0.14 µm/cycle and 0.12 µm/cycle, respectively. The growth rate of IMC grains diameter increases with the decrease of the solder ball diameter. After the ninth reflow cycle, the lateral growth rate of IMC grains begins to surpass the longitudinal growth rate. This phenomenon is more pronounced in the small-sized solder ball.

(3) The average Cu concentration in the solder bump increases with the number of reflow cycle increases and the Cu concentration in the small-sized solder ball rises more rapidly. The Cu concentration in the solder bump with ball diameter of 200 µm reaches a supersaturated state after the fifth reflow, while the Cu concentration with solder ball diameter of 800 µm is 1.553 wt%, which do not reach a saturated state. This is a direct kinetic control factor that produces size effect.

(4) The addition of Cu element in solder promotes the ripening reaction of IMC grains results in the increase of IMC lateral growth rate. Cu_6Sn_5 small particles at the Sn–0.7Cu/Cu interface hinder the grain boundary motion and inhibit the grain annexation.

Acknowledgements This work was supported by the National Natural Science Foundation of China (Grant Nos. 51871040 and 51571049) and "Research Fund for International Young Scientists" of National Natural Science Foundation of China (Grant No. 51750110504).

References

1. A.S.M.A. Haseeb, Y.M. Leong, M.M. Arafat, Intermetallics **54**, 86–94 (2014)
2. L. Liu, Z. Chen, C. Liu et al., Intermetallics **76**, 10–17 (2016)
3. C.W. Chen, T.C. Chiu, Y.T. Chiu et al., Intermetallics **85**, 117–124 (2017)
4. S.S. Ha, J.K. Jang, S.O. Ha et al., Microelectron. Eng. **87**(3), 517–521 (2010)
5. J.H. Lau, Microelectron. Ind. **28**(2), 8–22 (2011)
6. C.C. Chang, Y.W. Lin, Y.W. Wang et al., J. Alloys Compd. **492**(1–2), 99–104 (2010)
7. H.T. Ma, H.R. Ma, A. Kunwar et al., J. Mater. Sci.: Mater. Electron. **29**(1), 602–613 (2018)
8. W.K. Choi, H.M. Lee, J. Electron. Mater. **29**(10), 1207–1213 (2000)
9. H. Ma, A. Kunwar, R. Huang et al., Intermetallics **90**, 90–96 (2017)

10. L. Gu, L. Qu, H. Ma et al., ICEPT, 1–4 (2011). https://doi.org/10.1109/ICEPT.2011.6066848
11. H.K. Kim, K.N. Tu, Phys. Rev. B **53**(23), 16027 (1996)
12. L. Qu, H.T. Ma, H.J. Zhao et al., Appl. Surf. Sci. **305**(12), 133–138 (2014)
13. S. Li, Y. Du, L. Qu et al., ICEPT, 937–939 (2014)
14. M.L. Huang, F. Yang, N. Zhao et al., Mater. Lett. **139**, 42–45 (2015)
15. L. Qu, N. Zhao, H.J. Zhao et al., Scripta Mater. **72–73**(2), 43–46 (2014)
16. H. Ma, A. Kunwar, Z. Liu et al., J. Mater. Sci.: Mater Electron. **29**(6), 4383–4390 (2018)
17. Y. Zhu, F. Sun, Solder. Surf. Mt. Technol. **29**(2), 85–91 (2017)
18. C.M.L. Wu, M.L. Huang, J. Electron. Mater. **31**(7), 828–828 (2002)
19. X.P. Li, J.M. Xia, M.B. Zhou et al., J. Electron. Mater. **40**(12), 2425 (2011)